ABS4TSO - Extended Field Tests

Report on the extended field test period from
September 2022 to August 2023

Project team:

AIT Austrian Institute of Technology:	Christian Seitl, Adolfo Anta, Denis Vettoretti
Austrian Power Grid:	Viktor Zeh, Alexander Stimmer, Manuel Froschauer, Martin Lenz
VERBUND Hydro Power:	Klaus Oberhauser

Rev. 5
February 2024

Contents

1 Introduction

This report focuses on the results of the extended field tests conducted as a continuation of the ABS4TSO project. For a comprehensive overview of the ABS4TSO project, readers are encouraged to read the final report of the project [1]. The tests utilized a 1 MW, 500 kWh battery energy storage system with the possibility to activate and parameterize various functions dedicated to grid stability.

The primary aim of extending the ABS4TSO project, spanning from September 2022 to August 2023, was to conduct an in-depth assessment of the Synthetic Inertia (SI) as well as Frequency Containment Reserve+ (FCR+) and Enhanced Frequency Response (EFR) functionalities. Both, single- and multi-modal operations were performed.

In the power system, inertia plays a crucial role in maintaining grid stability by resisting changes in frequency during variations in power generation and/or consumption. Synthetic Inertia refers to the capability of power electronic devices emulating the stabilizing effects of traditional rotating masses found in synchronous generators' proving power in direct proportion to the Rate of Change of Frequency (RoCoF).

FCR+ represents a faster version of the current FCR and is designed to also replace a portion of the current FCR power. EFR represents a fast frequency-control-service designed to mitigate large frequency excursions caused by events with high power imbalances; the main purpose of EFR is to stabilize the system and support FCR during large frequency excursions. Both functions basically produce an output power proportional to the frequency, but with different dead-bands and 'end values' where full activation with maximum power is reached, and therefore, they are implemented as one function with different parameters.

Additional attention was given to the RoCoF values from different sources. On the one hand to better interpret the SI-function behavior, and on the other hand to evaluate the feasibility to use RoCoF values as direct input for a SI-function.

2 Test Parametrizations

Various parameter sets were utilized to investigate how these functions perform over an extended period. Table 1 shows a list of field tests carried out throughout the project. This report exclusively focuses on the tests executed during the project's extension phase (TEST-012 to TEST-017). Prior tests were already analyzed within the ABS4TSO final report [1]. Beside the field tests, lab and CHIL tests were undertaken within the original project, testing other functions (APC, RPC, DFD, FS, etc.) and parametrizations (EFR-1 to EFR-8, SI-1 to S-10, etc.). Table 3 and 2 show the parameters of each test. For a detailed explanation of the parameters meanings see [1].

Field Test	APC	RPC	DFD	EFR	FS	PSS	SI	SR	Datetime (optional)
TEST-001	-	-	-	EFR-9	-	-	-	SR-1	October 18, 2021
TEST-002	-	-	-	EFR-10	-	-	-	SR-1	October 25, 2021
TEST-003	-	-	-	-	-	-	SI-11	SR-1	November 1, 2021
TEST-004	-	-	-	-	-	-	SI-15	SR-1	November 8, 2021
TEST-005	-	-	-	EFR-11	-	-	-	SR-1	November 15, 2021
TEST-006	-	-	-	EFR-12	-	-	-	SR-1	November 22, 2021
TEST-007	-	-	-	-	-	PSS-1	-	SR-1	November 29, 2021
TEST-008	-	-	-	EFR-13	-	-	SI-16	SR-1	December 6, 2021
TEST-009	-	-	-	EFR-14	-	-	SI-16	SR-1	December 13, 2021
TEST-010	-	-	DFD-7	-	-	-	-	SR-1	December 20, 2021
TEST-011	-	-	-	EFR-13	-	-	SI-17	SR-1	December 27, 2021
TEST-012	-	-	-	EFR-7	-	-	-	SR-1	September 7, 2022
TEST-013	-	-	-	EFR-11	-	-	-	SR-1	November 8, 2022
TEST-014	-	-	-	-	-	-	SI-19	SR-1	December 20, 2022
TEST-015	-	-	-	-	-	-	SI-20	SR-1	January 27, 2023
TEST-016	-	-	-	EFR-15	-	-	SI-5	SR-1	February 23, 2023
TEST-017	-	-	-	EFR-16	-	-	SI-20	SR-1	May 19, 2023

Table 1: Used parametrization during the field tests

Param.	EFR-7	EFR-11	EFR-15	EFR-16
P	1000.0	1000.0	500.0	1000.0
dF_max	0.200	0.200	0.200	0.200
DeadB	0.010	0.050	0.010	0.010
Thres	100.0	100.0	100.0	100.0
Tact	0.000	0.000	0.000	0.000
Tfull	0.000	0.000	0.000	0.000
Thold	1800.0	1800.0	1800.0	1800.0
Tback	0.0	0.0	45.0	45.0
Toff	0.0	0.0	180.0	180.0

Table 2: Used parameters for EFR-function

Param.	SI-5	SI-19	SI-20
P	500.0	1000.0	1000.0
H	98.0	98.0	98.0
Ramp	60.0	60.0	60.0
DBf	0.000	0.010	0.000
DB	0.010	0.002	0.010
thres	0.010	0.000	0.010
grad	1.000	1.000	1.000
tact	0.000	0.000	0.000
Inakt_En	1.000	1.000	1.000

Table 3: Used parameters for SI-function

3 Single-Modal Operation

This chapter covers TEST-012 to TEST-014 where one function was tested over a longer period. Tests 001 to 011 had been discussed in the report of the original project. Chapter 4 will cover tests where two functions were activated at the same time.

3.1 TEST-012

For *TEST-012* the main objective was to test the Frequency Containment Reserve+ (FCR+) function over a longer period. A detailed description of its principle of operation can be found in the ABS4TSO final report [1] of the original project.

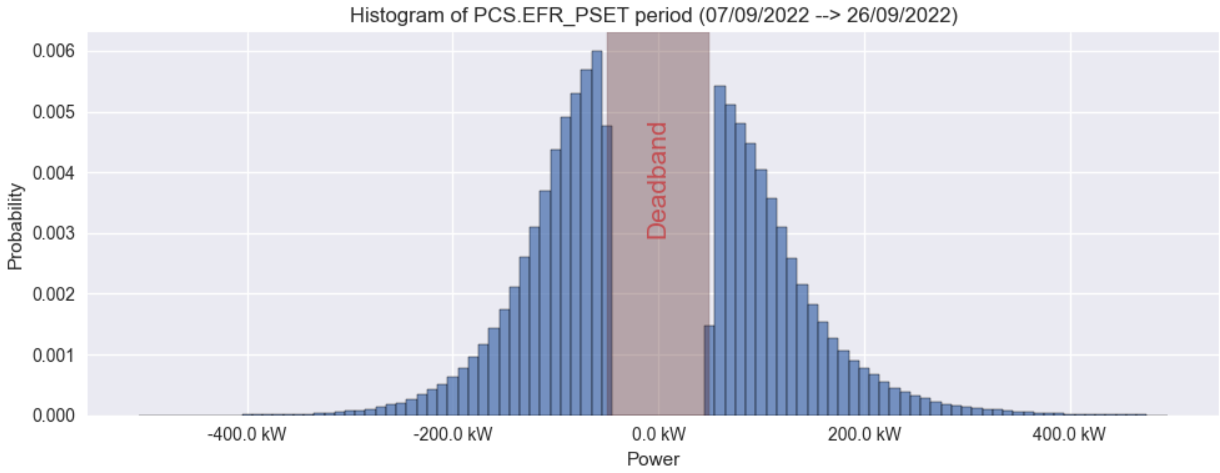

Figure 1: FCR+ active power set-points histogram with EFR-7 parametrization over 19 days in September 2022.

Figure 1 shows a histogram of the FCR+ active power set-points. This matches the frequency distribution of the period. The system provides primary frequency response with a dead-band of $\pm 10\,\mathrm{mHz}$. Various transient responses were analyzed manually. This three week test showed that the system was able to keep the state-of-charge of the batteries within a specific band all the time, while completely fulfilling the demands of the FCR+ function.

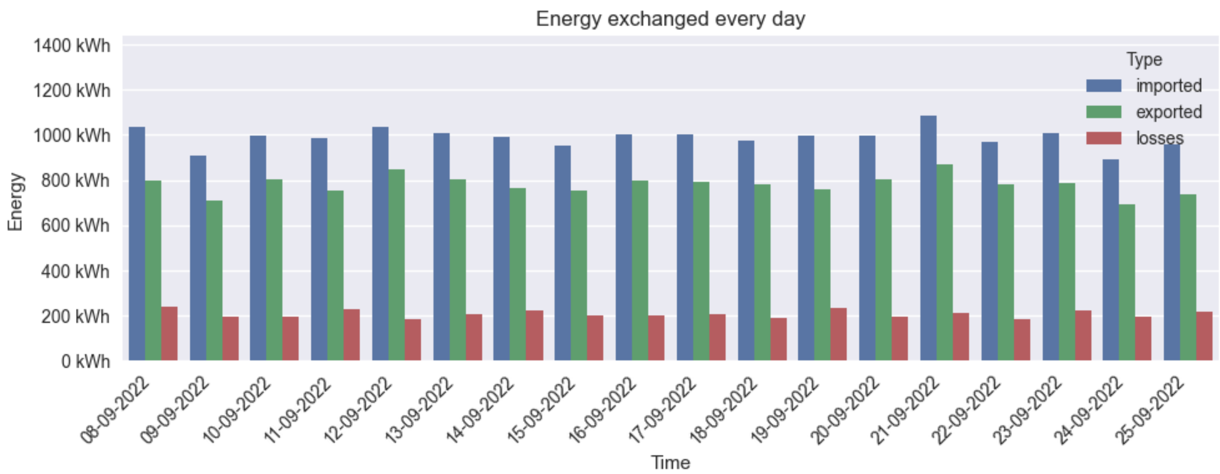

Figure 2: Daily energy exchange for FCR+ with EFR-7 parametrization.

Figure 2 shows the imported and exported energy as well as the losses for every day throughout the test. With the given very sensitive parametrization, the system had an energy exchange of roughly two cycles every day, which is an important information for the life time of the system. The daily energy throughput of ≈ 800 kWh was approximately 8% of the the maximum of roughly 12 MWh, whereby the nominal power of the system is 1 MW. The system was either in standby or operating at partial load with corresponding low inverter efficiency. This lead to an overall energy efficiency of around 80%. While this seems quite low at first glance, the losses were much higher in the following tests, where standby predominated.

3.2 TEST-013

The primary goal of *TEST-013* was to assess the performance of the EFR function over a longer period. A detailed description of the EFR can be found in the ABS4TSO final report [1] of the original project. In contrast to FCR+, EFR has a frequency dead-band resulting in no operation for most of the time. The underlying concept is that EFR will activate only when significant frequency deviations occur. In the original description of EFR a dead-band of ± 200 mHz was defined. As this would have resulted in hardly any activations, a smaller dead-band of ± 50 mHz was defined for this test.

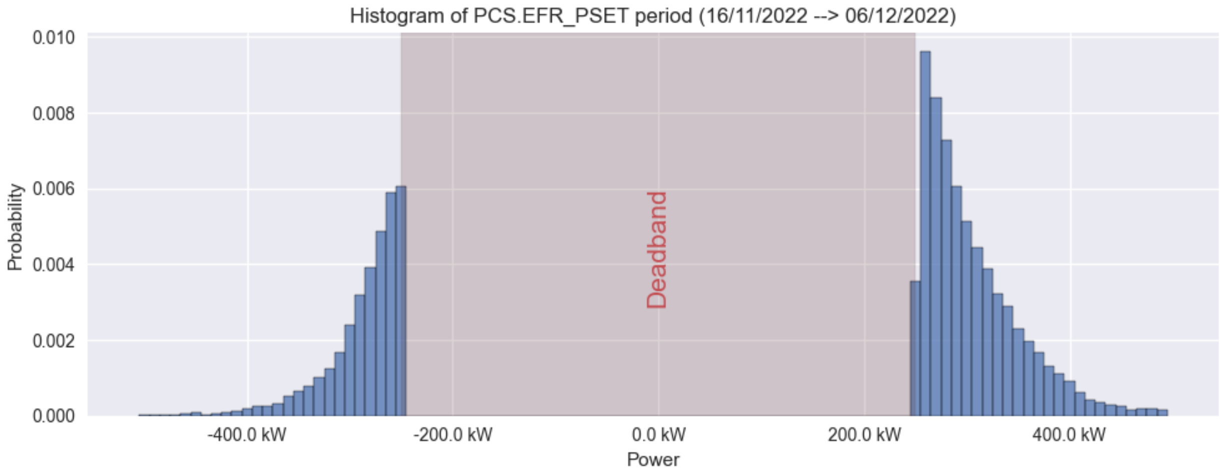

Figure 3: EFR active power set-points histogram with EFR-11 parametrization.

Figure 3 shows a histogram of EFR function's active power set points. The frequency dead-band of ± 50 mHz lead to a power dead-band of ± 250 kW. The function remained inactive for most of the time as the grid frequency was within the 50 ± 0.05 Hz band. This was also observable when examining the overall system energy exchange (cf. Figure 4). As the inverter was predominantly in an idle or "hot standby" state, it operated at a very inefficient operating point: it discharged the battery only to cover inverter and transformer losses, which caused substantial losses. Despite the high losses, the system showed its capability of continuously providing Enhanced Frequency Response.

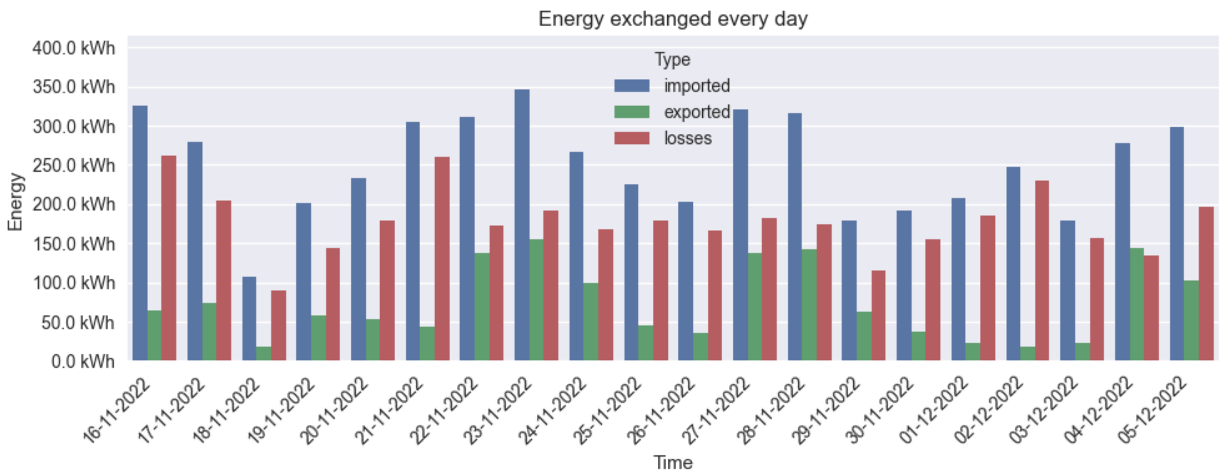

Figure 4: System efficiency with EFR-11 parametrization.

3.3 TEST-014

TEST-014 tested the SI function with realistic parameters over a long period of time. Because frequency events with a high RoCoF - which would then lead to an activation of the function - are not very common, the field test period of the original project could not catch relevant SI-events to validate the performance of the system.

Figure 5 shows a histogram of the SI-function's active power set points. The bin at 0 kW was removed as it would dominate the whole figure and would recognize all the other bins as zero. This figure, as well as the daily energy exchange in Figure 6, show that the function was not active for most of the time. The system produced almost only losses, slowly discharging the battery until the state-of-charge (SoC) went beyond the specified threshold and the system controller charged the battery.

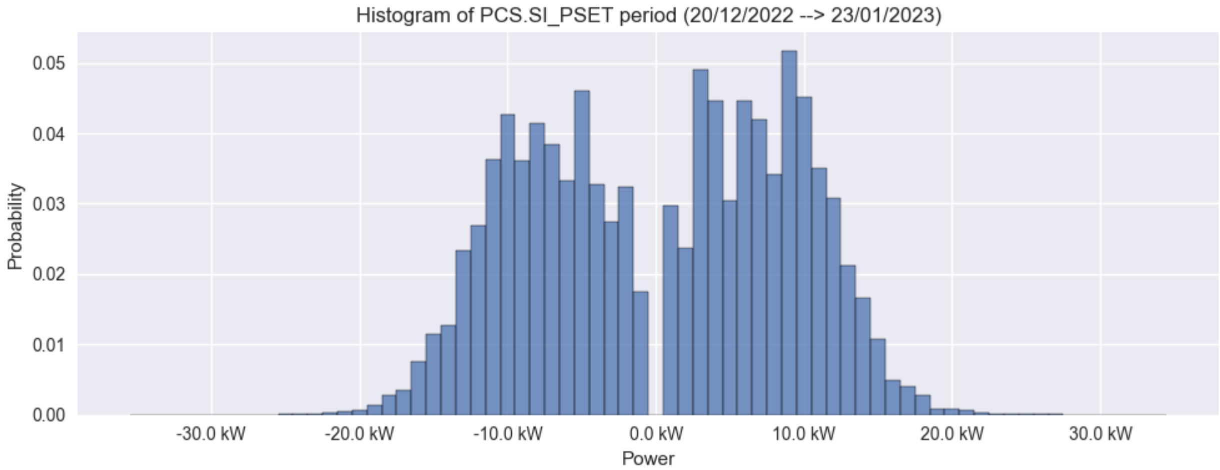

Figure 5: SI active power set-points histogram with SI-19 parametrization, zero power filtered for scaling reasons

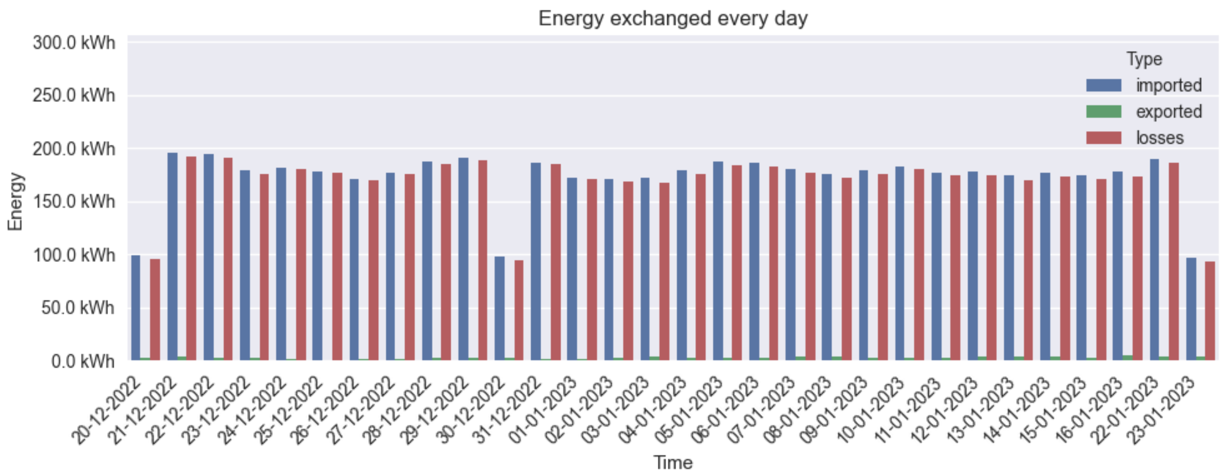

Figure 6: Daily energy exchange over a one month SI test period with SI-19 parametrization.

Only two SI-events worth mentioning occurred in the one month test period, shown in Figure 7 and Figure 8. The dead-band was set to ± 10 mHz, indicating the systems internal RoCoF values must have exceeded this value. Unfortunately it was not possible to read this internally calculated value. To get an idea of how the RoCoF value looked during these events, an ex post calculated RoCoF was added to the figure (difference of the moving average over five 100 ms-frequency measurement values). For a potential future product or future grid code requirement, the authors recommend that the systems shall provide their internal RoCoF values as they already do for power or frequency measurements.

Given the nominal power of the system of 1000 kW, the accuracy of MV-sensors and the small output power of the function, it is challenging to distinguish the function's behavior from measurement noise and the general ability of the system to provide a certain set point at the MV side below 1% of nominal power.

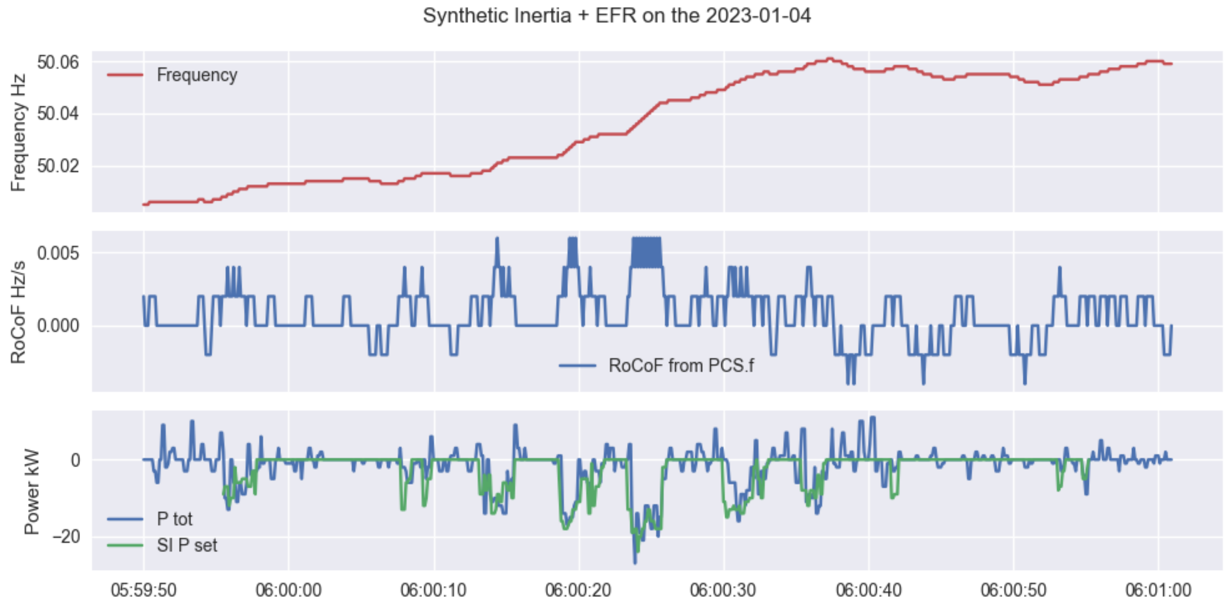

Figure 7: SI event on the 2023-01-04 with SI-19 parametrization.

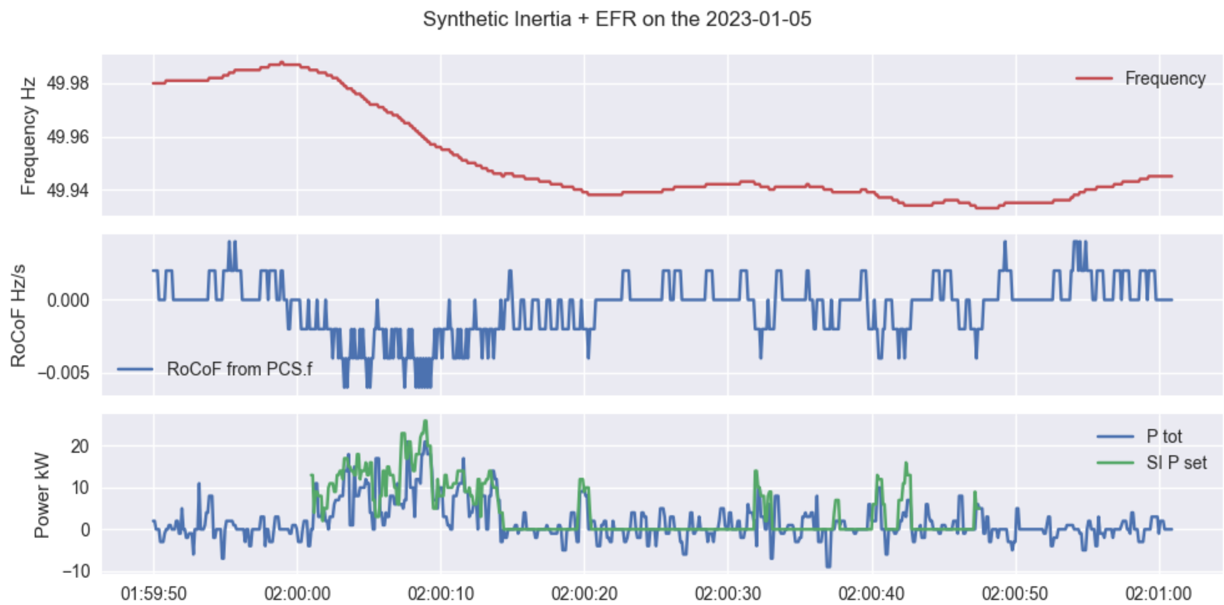

Figure 8: SI event on the 2023-01-05 with SI-19 parametrization.

3.4 TEST-015

With *TEST-015*, the primary aim was to repeat SI-function tests with an increased likelihood of detecting frequency events while at the same time improving noise rejection. Using the SI-20 parametrization, the frequency dead-band was set to 0 mHz, allowing the SI to respond to events, even when the frequency was very close to its nominal value. To prevent the SI function from reacting to noise, the RoCoF dead-band was extended to 10 mHz/s.

The SI power set-points histogram and system efficiency of this test were not included, as they closely resemble the data presented in Figure 5 and Figure 6. As expected, even with a more sensitive parametrization, the system was in hot standby for most of the time, leading to repeated battery discharge and charge. A suggestion to overcome this issue is given in Section 6.

During the observation period, four events were recorded. The results of those are reported in Figures 9 to 12. It can be noted that compared to *TEST-014*, the noise level was reduced due to a higher RoCoF dead band of 10 mHz/s compared to 2 mHz/s (c.f. Figure 9-11). Also, the output power of the SI function closely resembled the system output highlighting the correlation between frequency, RoCoF and SI set-points. Finally, the SI function's behaviour was better aligned with the offline simulations and the theoretical expectations.

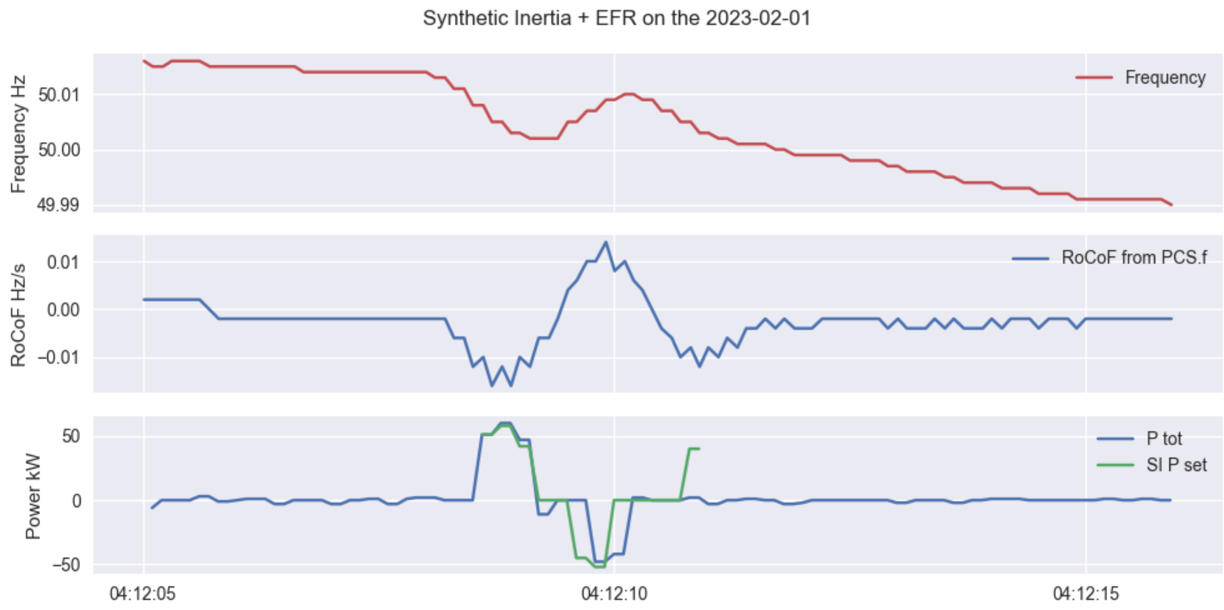

Figure 9: SI event on the 2023-02-01 with SI-20 parametrization.

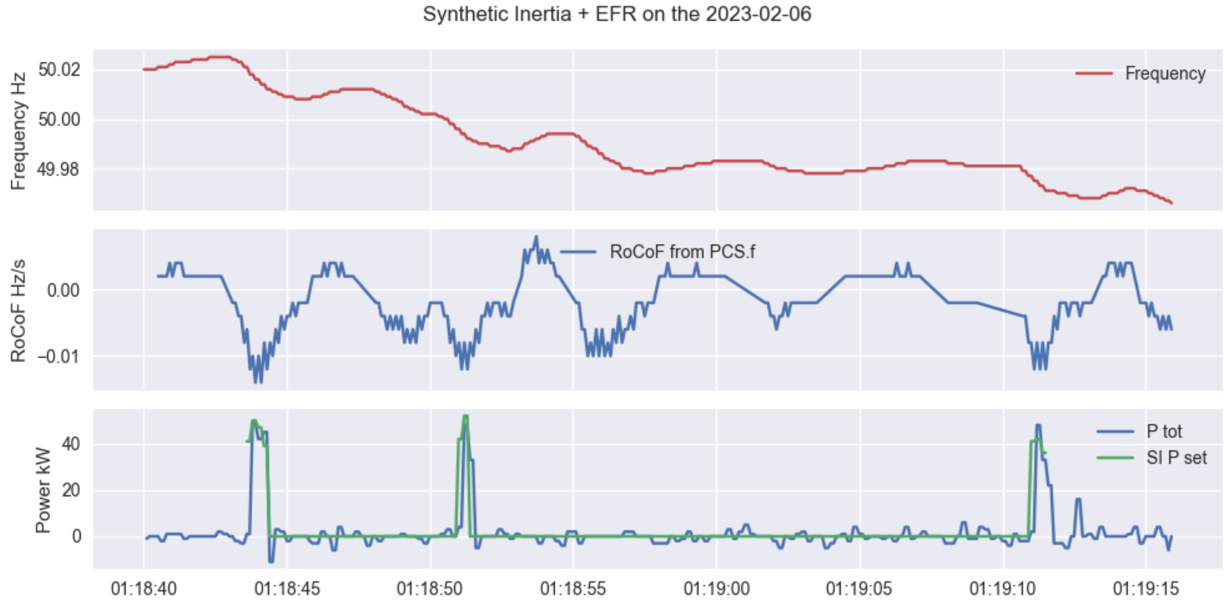

Figure 10: SI event on the 2023-02-06 with SI-20 parametrization.

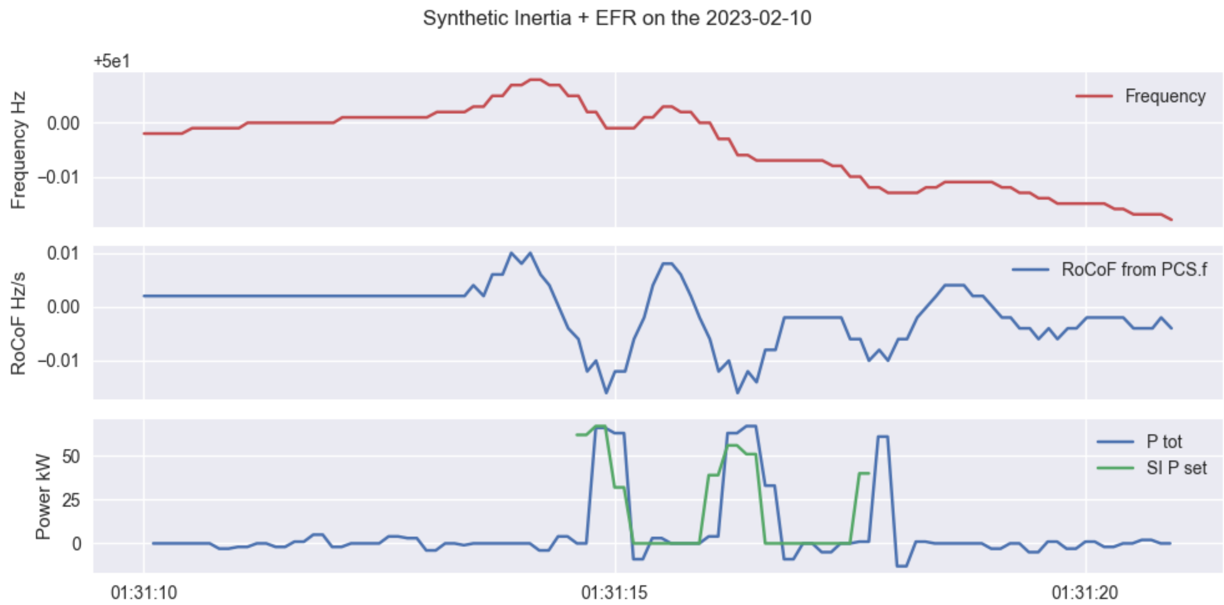

Figure 11: SI event on the 2023-02-10 with SI-20 parametrization.

Figure 12 shows the frequency event occurred on 19th February 2023. On this day there was a low frequency oscillation with a cycle time of ≈0.5 Hz, causing the SI-function to respond to it (c.f. Figure 13 which shows a FFT of the frequency). Such low frequency oscillations can in principle be present in the grid as inter-area or local modes. Ideally, the response of the SI-function to this low frequency oscillation should be zero because it should react only to larger frequency deviations.

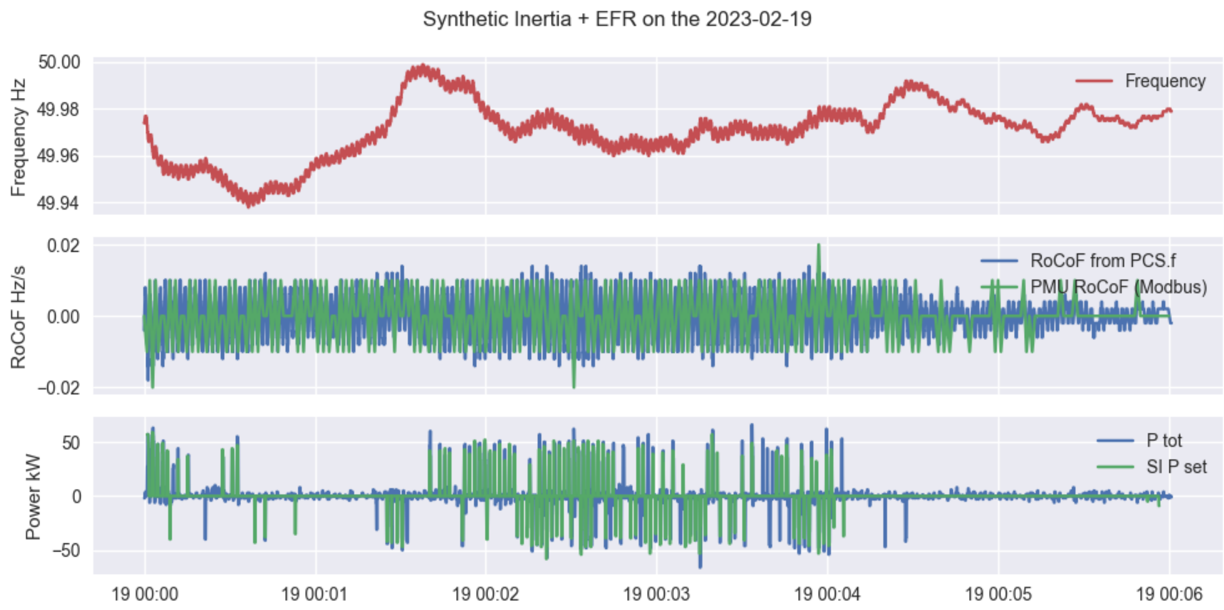

Figure 12: SI event on the 2023-02-19 with SI-20 parametrization.

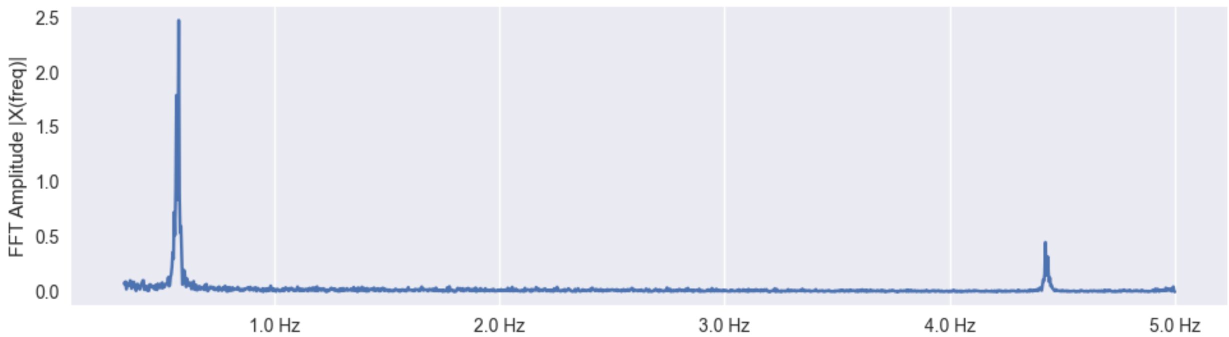

Figure 13: FFT of the PCS frequency on the 2023-02-19.

Because the SI parametrization is very sensitive, even small RoCoF events cause system responses. Having multiple batteries responding in this way is not beneficial for the grid and it can cause grid instabilities. However, using a less sensitive parametrization might result in the SI failing to respond to larger frequency deviations, rendering it ineffective. Therefore, selecting the appropriate parametrization to align with the expected theoretical behavior is a challenging task; the experience gained during field tests revealed that it is still not totally clear if and how this can be done as a general rule for multiple systems from multiple manufactures located at various positions in the grid.

4 Multi-Modal Operation

The aim of testing multi-modal operation was to determine whether the system is feasible for taking advantage of the capabilities of different functions simultaneously.

4.1 TEST-016

At *TEST-016* the SI- and FCR+/EFR-function were enabled at the same time. To avoid that the active power set-point exceeded the physical limit, the maximum power of EFR and SI was limited each to the half of the nominal power. The daily energy exchange shown in Figure 14 matches the previous results of a FCR+/EFR parametrization (c.f. Figure 2 and Figure 4). The additional activation of SI is not worth mentioning in the context of imported/exported energy.

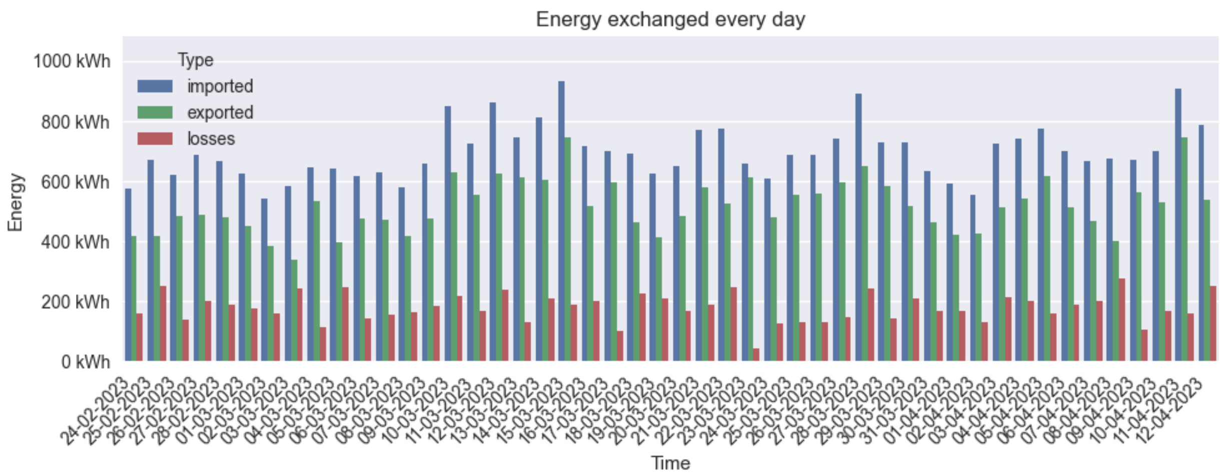

Figure 14: Daily energy exchange in multi-modal operation with SI-5 and EFR-15 parametrization.

During the test period a few frequency events occurred. The two most relevant are shown in Figure 15 and Figure 16. For more insights of the behaviour, the RoCoF values from an Arbiter PMU - installed directly inside the system - are added in the figures.

Of particular interest is the combined behaviour of SI and EFR in Figure 15 where at 06:55:52 the SI function set-point was in contrast with the EFR set-point. Since the frequency was above the nominal value of 50 Hz the EFR function set-point was negative and the battery was charging. The grid frequency had an oscillation and the RoCoF at that particular time was negative, thus the SI set-point was positive. The total battery set-point is computed as the sum of the the SI and EFR set-points and as a consequence, the output power was lowered.

For this specific use-case the EFR set-point was dominant making the effect of SI negligible. Nevertheless, this aspect should not be disregarded, as in a situation where primary frequency response and synthetic inertia are widely adopted, it could potentially lead to undesirable behaviors. Frequency oscillations lead to an unwanted oscillatory response of the SI function. A possible adaption could be that the SI-function should provide power only in one direction based on the deviation of the frequency from the nominal value. If the grid frequency is above 50 Hz, the SI set-point should always be negative (or zero) and vice versa.

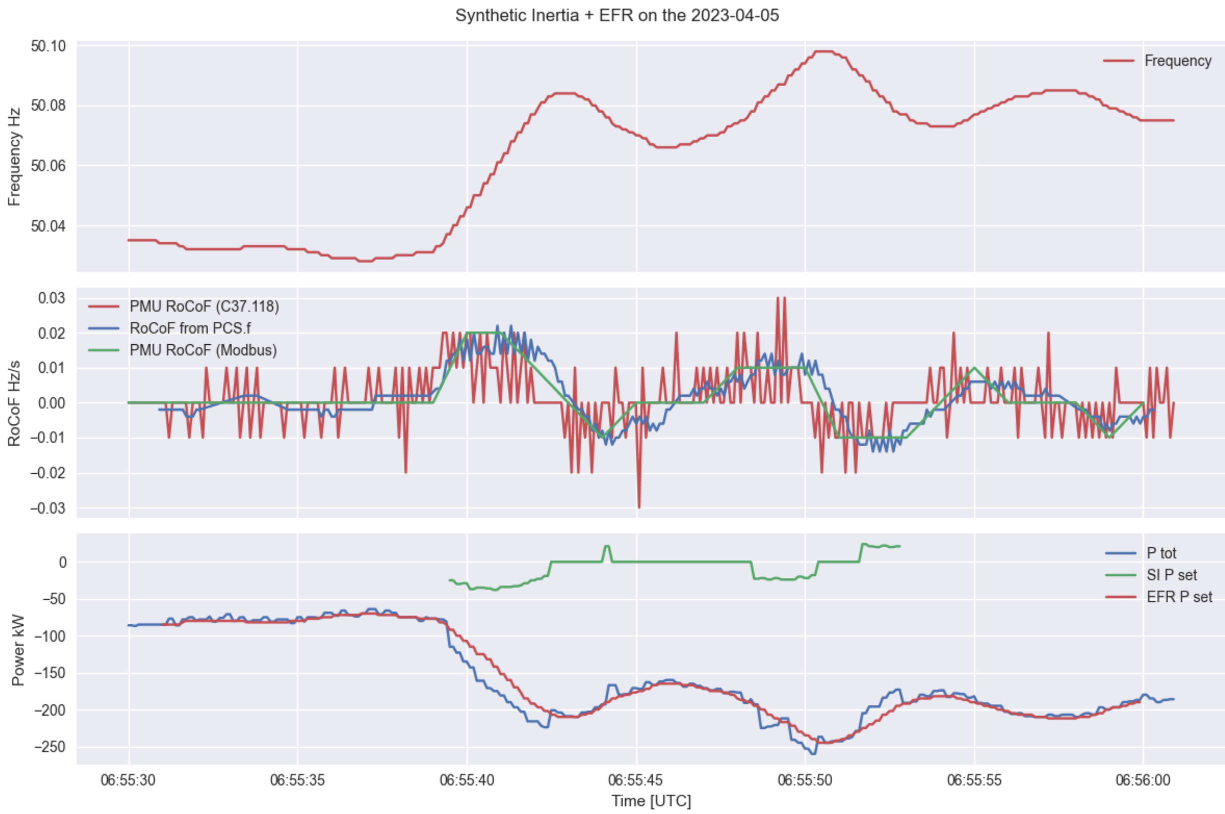

Figure 15: SI event 2023-04-05

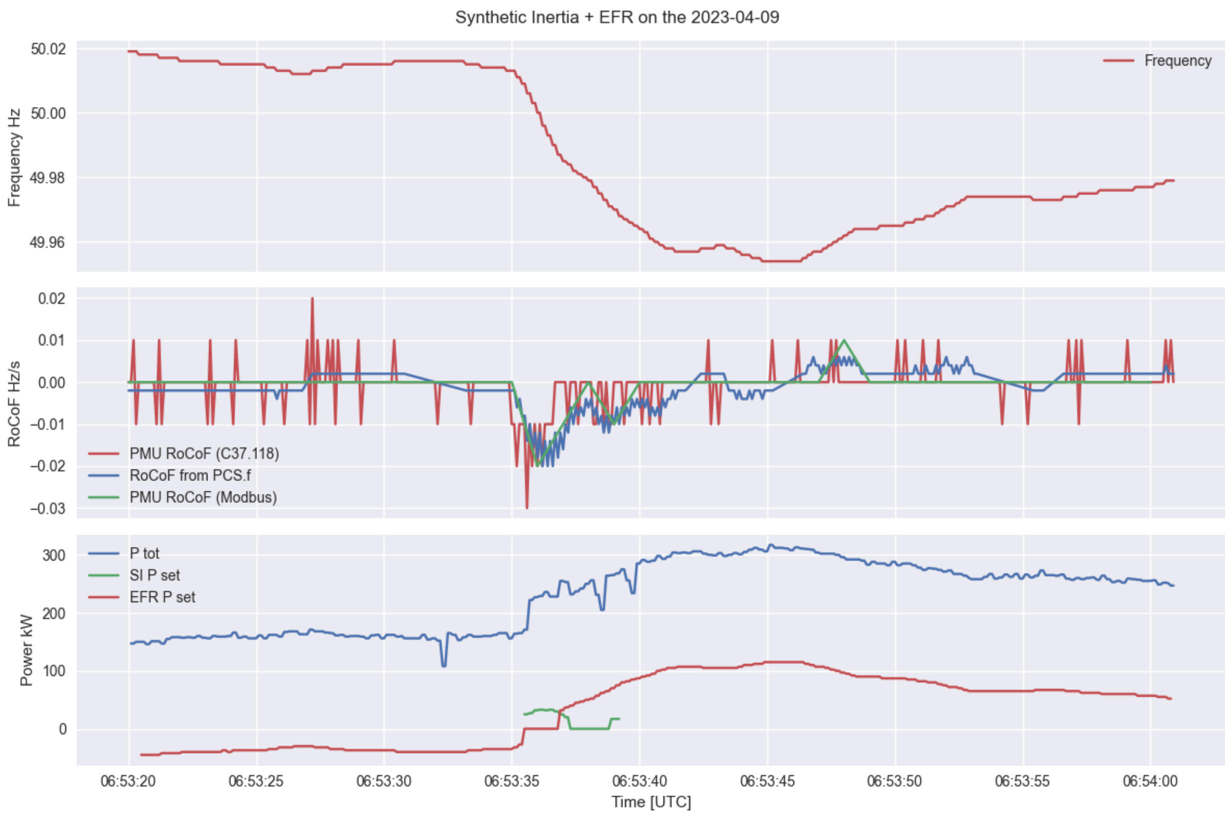

Figure 16: SI event 2023-04-09.

4.2 TEST-017

As in the previous multi-modal test, the goal of this test was to assess the simultaneous operation of the system with both SI and EFR enabled. In comparison to the previous one, the maximum power set-point for both functions was set to 1 MW. This can potentially lead to a scenario in which the combined active power set-point for SI and EFR exceeds the physical limit of the systems nominal power.

The daily energy exchange shown in Figure 17 shows the same results as the one of *TEST-016*. In Figure 18

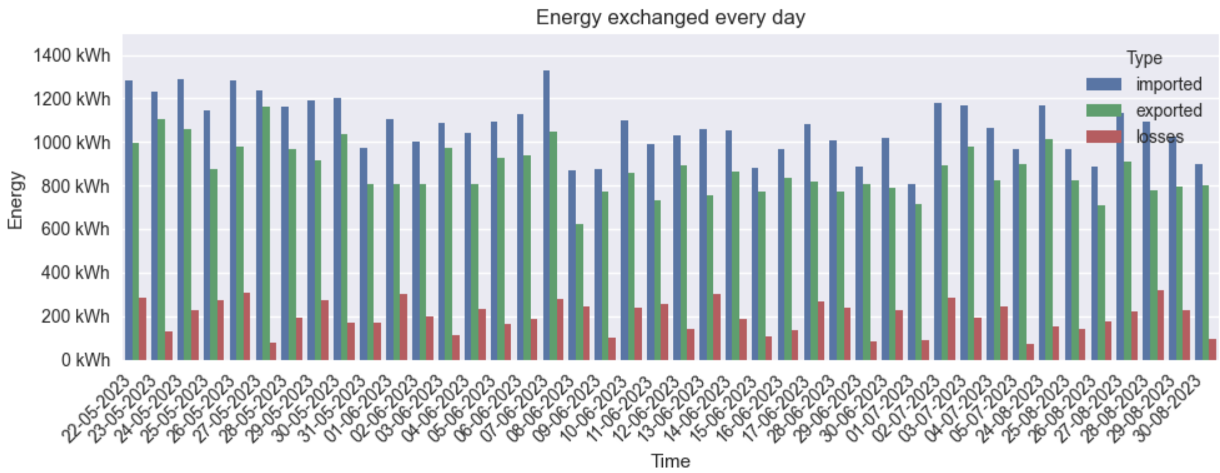

Figure 17: Daily energy exchange in multi-modal operation with SI-20 and EFR-16 parametrization.

and Figure 19 show the two most relevant SI-events. Similar to Figure 15, the set-points of SI and EFR have different signs. This happened at 10:28:32 where the RoCoF was negative and thus the SI set-point was positive. Beside this, the grid frequency was above the nominal value of 50 Hz leading to a negative EFR set-point (battery charging). The same considerations reported in *TEST-016* are valid also in this case.

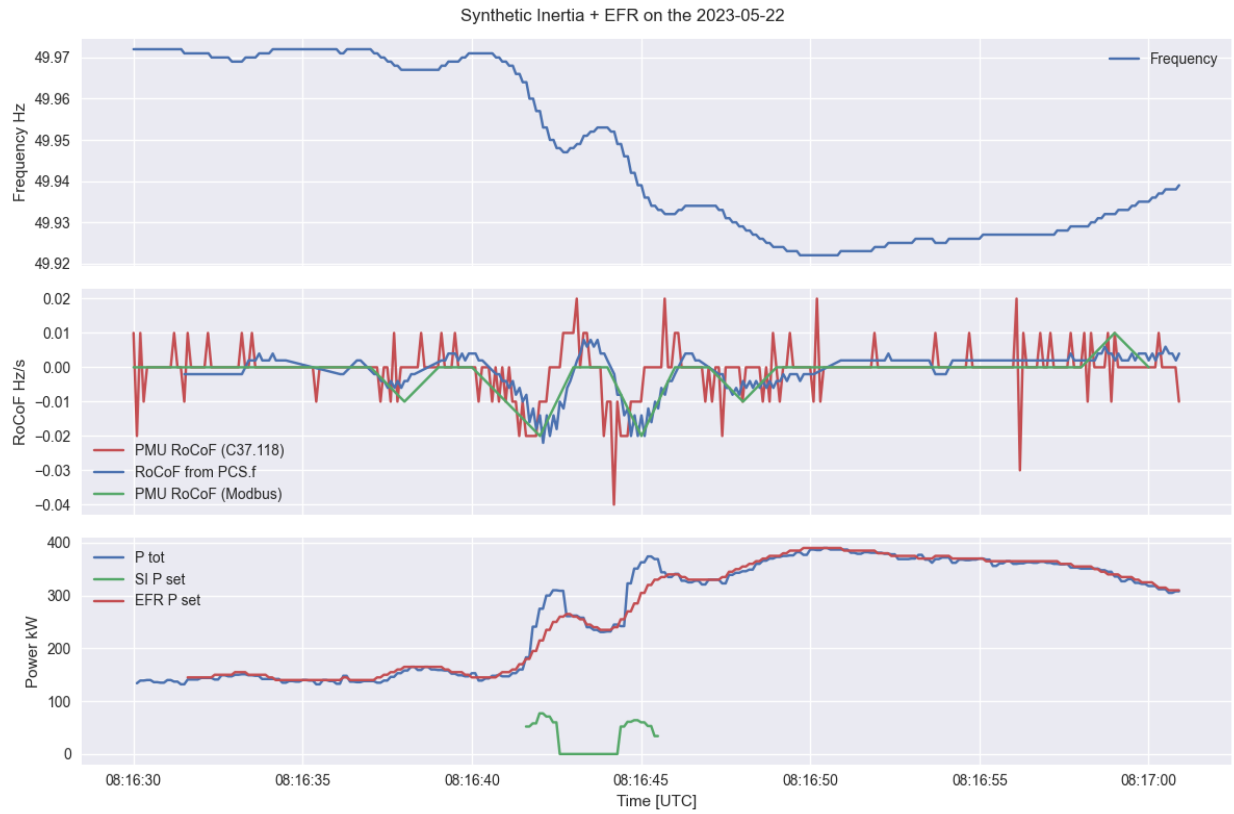

Figure 18: SI event 2023-05-22.

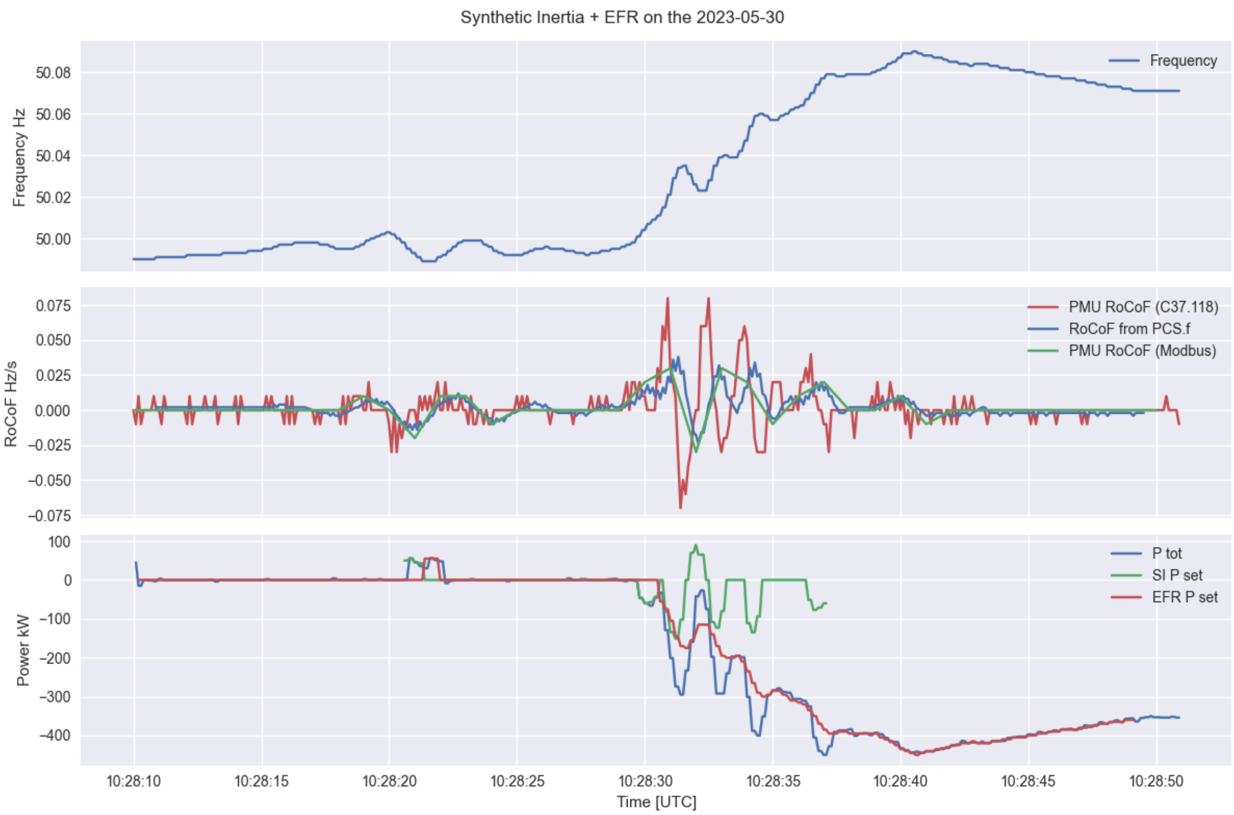

Figure 19: SI event 2023-05-30.

4.3 Simultaneousness Analysis

To investigate potential issues that the combined maximum power of the activated functions exceed the nominal power, two so called violin plot were created, as shown in Figure 20 and 21. The left violin plots in the figures cover the period of *TEST-016*, while right violin plots cover *TEST-017*. The red marks inside the plots represent the daily minimum and maximum power peaks. A random jitter on the x-axis was added to be able to distinguish between the various dots. The filled curves show an estimation of a probability density function of those daily minimum and maximum power peaks.

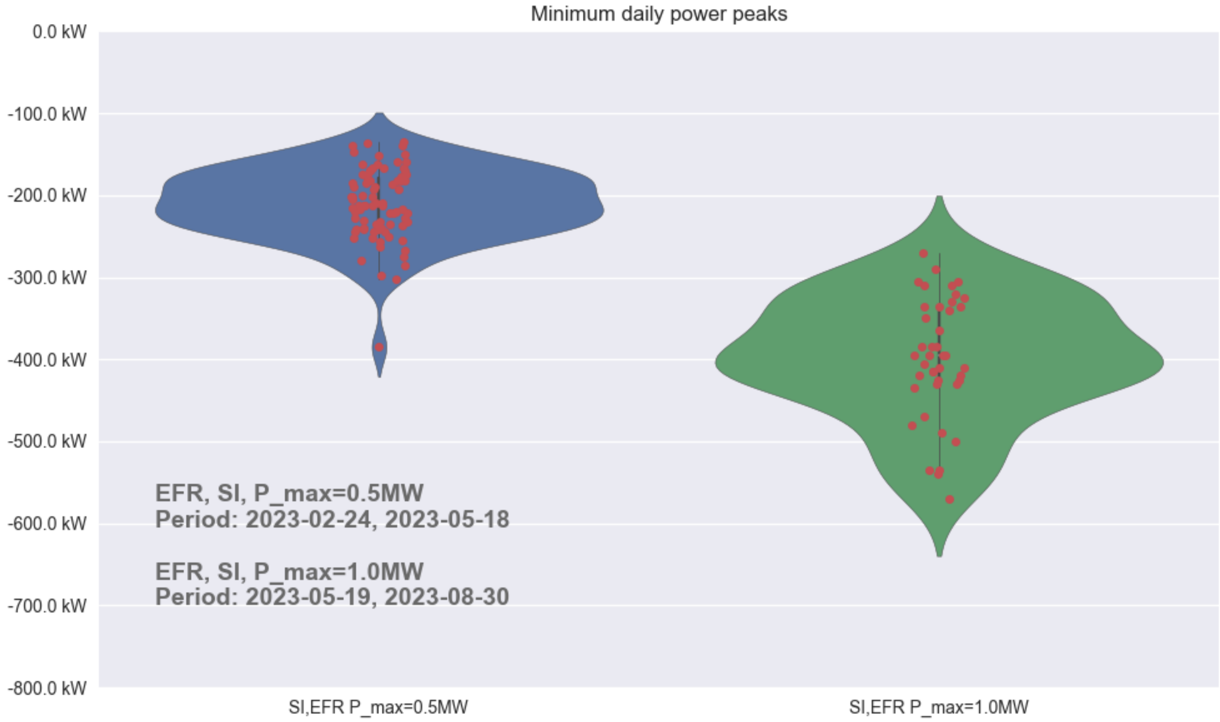

Figure 20: Minimum daily power peak of the battery system computed as sum of the SI and EFR power set-points.

The four "violins" show that the ends of this estimated distribution are far from the maximum of 500 kW and 1000 kW respectively. Although this is just an estimation over a couple of dozens of samples, it provides a good impression on the simultaneousness of the two functions.

As future work, the authors suggest conducting a theoretical worst-case analysis, such as a system split with high imbalance in all islands, as well as some offline simulations with measurements of critical grid events from the past. This work could confirm the hypothesis of a possible "overload" of the parametrization.

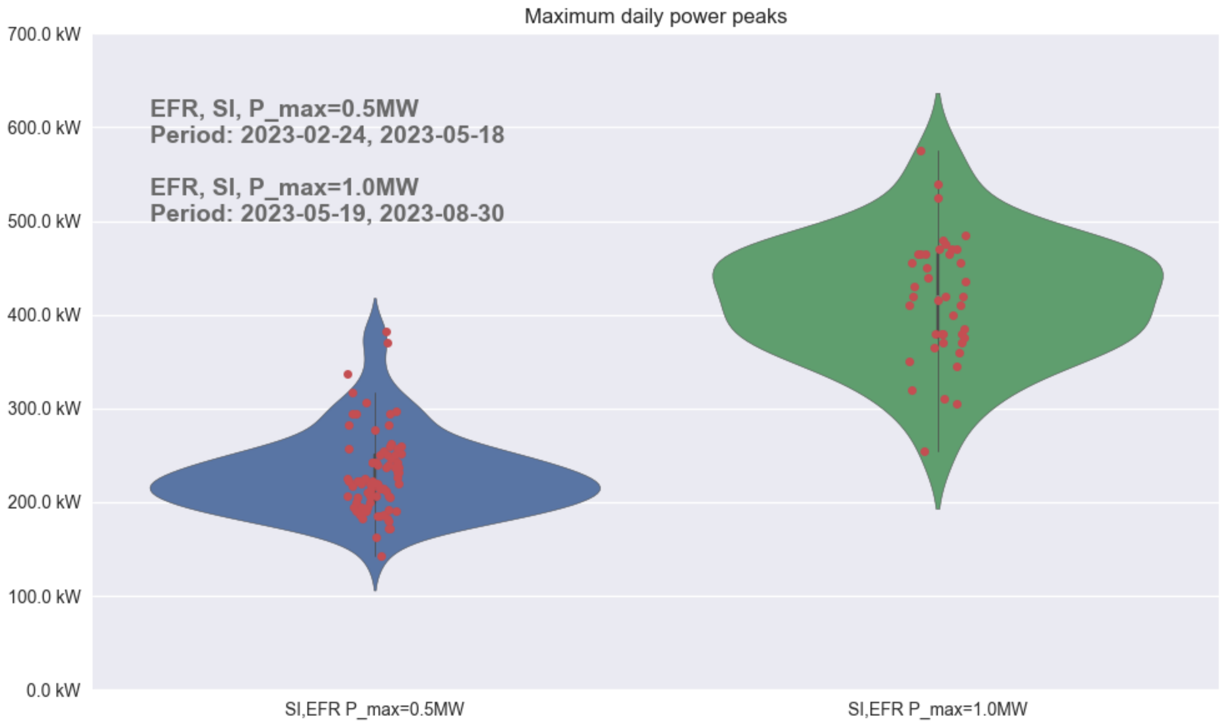

Figure 21: Maximum daily power peak of the battery system computed as sum of the SI and EFR power set-points.

5 Comments on RoCoF Values in the Context of the SI-Function

During the field tests, the question arose whether RoCoF values from PMUs, or RoCoF values calculated from frequency measurements (e.g. from a power quality measurement device) could be used as an input for the SI-function. However, this promising idea turned out not to work.

First the authors analyzed values from an Arbiter PMU [3] mounted directly at the MV connection of the system. The resolution of the PMU's values is 10 mHz/s, which is far too small to calculate SI function responses out of those values. The low resolution is probably due to the requirements of the IEEE Standard for Synchrophasors for Power Systems (IEEE C37.118) [2] that request an accuracy of 10 mHz/s. Additionally, there is a limited update rate. Via the C37.118 protocol, the Arbiter PMU provides an updated value only every 100 ms, for Modbus it is even 1 s. In addition to the slow update rate, the communication link itself adds latency. This delays can have the effect that the natural oscillation of the grid frequency and the synthetic inertia as countermeasure are out of phase, making the situation possibly even worse. On top of the limited resolution and the latency issues, the present PMU lacked in providing a stable communication link, especially via its Modbus protocol. Therefore the PMU values were considered not suitable as an input for the SI-function.

The used storage system offers the possibility to read several internal measurements like the frequency with an update rate of 100 ms. This rate is higher than for most other known storage systems (typically 1 s). The authors tried several RoCoF calculations based on the difference of moving average values (noted in the figures as *RoCoF from PCS.f*). The values have been suitable for either getting a notion that a RoCoF event is happening; or determining the RoCoF in hindsight - but not suitable as input for an SI-function in real time.

Finally the authors utilized values from an *A. Eberle PQI-DA smart*. This quality measurement device provides half period frequency values via an interface that adds a latency of just 1 to 3 ms. This update rate is ten times higher than the others and should give the possibility to react faster to frequency changes with a better accuracy of the RoCoF values. But it turned out that every 300 ms the devices needs approx. 100 ms to respond to a read request, continuing with 1 to 3 ms for the next 30 values and then 100 ms respond time again. After some time, the manufacturer was able to find out the reason: a combination of the requirements of IEC-61000-4-30 with measurement values synchronous to zero-crossing and a mismatch between internal 200 ms buffer and multiples of the cycle times for any frequencies apart from 50 Hz. Since the maximum latency is around 100 ms, the devices falls into the same category as the mentioned above and not suitable for the SI-function too.

To sum it up, in theory it should be possible to use frequency values from (existing) external devices. But the requirements regarding update rate as well as latency are challenging and the three tested devices did not perform sufficiently. Therefore the authors recommend a dedicated filter/transfer function calculated within the inverter to determine the RoCoF value as input for the SI-function (which is how it the function implemented in the given system under test). Additionally to this, and as already mentioned in section 3.3, the authors recommend that internal RoCoF values shall be provided via a digital interface to allow accurate monitoring of the function.

6 Gained Knowledge and Conclusions

First of all, the FCR+/EFR tests showed that the system is able to continuously provide those functions over a longer period of time, including automatic re-charging of the battery to keep the state-of-charge in a specified band. This verification could not have been done within the original project due to time constraints. The particular parametrization of the FCR+ as well as EFR-function define the share between providing output power and staying in an "idle mode". This directly influences the share of losses and the imported/exported energy.

In the context of losses, it is worth to mention the general operating/control strategy, especially for functions whose output is most of the time zero. Currently, the output power set value is defined at the MV point of coupling. This set value is most of the time zero and power from the battery is necessary to cover inverter and transformer losses, resulting in a permanent discharge of the battery (with periodic re-charge). Additionally, at this operating point the efficiency of the inverter is quite low. This leads to unnecessary losses and aging of the battery. To overcome this, the authors recommend that those "hot standby losses" are covered from the AC side with the output set value of the functions on top of this losses. This would result in a "base load" with corresponding energy costs, but less SoC restoration events leading to less total losses.

As expected from the field tests of the original project, the experiences with the SI-function were ambivalent. The parametrization of the function is always a trade-off between sensitivity and robustness and it is difficult to find a sweet spot here. The tests also showed that a certain parametrization is not sensitive or robust per se. A parametrization can be robust against measurement noise but very sensitive to low frequency oscillations. Just doing more or longer tests is not sufficient to solve this issue. Luckily, there are hardly any events which lead to high RoCoF values that are significantly higher than the measurement noise. On top of this, there are multiple possible algorithms to determine an estimation for the derivative of the frequency and various "adjusting screws" within those algorithms. Another vector in this multi-dimensional optimization problem is the placement of the measurement itself, MV or LV, as well as the amount of harmonics. This could be tackled by extended CHIL-tests including also an realistic emulation of measurement noise.

The fields tests also addressed the question whether input values of other measurement devices (PMUs, power quality measurement devices, etc.) can be used as an input of the SI-function - either directly, e.g. the PMUs RoCoF value, or calculated from frequency values. Investigating the RoCoF values of a PMU installed within the system led to the conclusion that they are not suitable. This is because of the limited resolution of the values, which is 10 mHz/s and probably related to a required accuracy of 10 mHz/s according to C37.118 standard, as well as latency and long term communication stability. Using dedicated frequency measurements and calculating the "frequency derivative" via the difference of (moving) average values resulted in RoCoF values that helped to better understand the grid frequency behavior. But they are not utilizable as input of the SI-function for basically the same reason as mentioned above.

For multi-modal operation, two aspects can be mentioned. First, that EFR- and SI-function can have output values with opposite power directions resulting in a neutralization effect (c.f. Section 4.2). This unwanted behaviour can be tackled with a different parametrization or an extension of the SI-function (output value is not only depending on the RoCoF, but also if the grid frequency is above or below the nominal frequency). Complex function definition can lead to a behavior that is not completely understandable and predictable (by humans). However, an understanding of how the grid will react in certain failure scenarios is crucial for a safe and reliable operation.

Secondly, there is limited simultaneousness of the EFR- and SI-functions output values and a first statistical analysis showed a potential to "overload" the combined maximum power of the functions. Especially if the time for full activation of EFR is in the range of some seconds. Nevertheless, it has to be taken into account that the grid must be prepared for the rare worse cases with a high RoCoF (e.g. system split with high imbalance in the islands) and not for the most probable cases.

References

[1] Alexander Stimmer et al. *Advanced Balancing Services for Transmission System Operators (ABS4TSO) - Publizierbarer Endbericht*. 2022. URL: https://energieforschung.at/wp-content/uploads/sites/11/2018/05/ABS4TSO_Publizierbarer_Endbericht_FINAL.pdf.

[2] "IEEE Standard for Synchrophasor Measurements for Power Systems". In: *IEEE Std C37.118.1-2011 (Revision of IEEE Std C37.118-2005)* (2011), pp. 1–61. DOI: 10.1109/IEEESTD.2011.6111219.

[3] *MODEL 1133A POWER SENTINEL GPS-SYNCHRONIZED POWER QUALITY REVENUE STANDARD*. URL: https://www.arbiter.com/files/product-attachments/1133a_manual.pdf.